NUMERICAL SIMULATIONS OF A FULLY DEVELOPED TURBULENT CHANNEL FLOW BY FINITE ELEMENTS

Jorge D'Elía[*], **Gerardo Franck**[†*]**, Mario Storti**[*]**and Norberto Nigro**[*]

[*]Centro Internacional de Métodos Computacionales en Ingeniería (CIMEC)
Instituto de Desarrollo Tecnológico para la Industria Química (INTEC)
Universidad Nacional del Litoral - CONICET
Parque Tecnológico Litoral Centro (PTLC) s/n, 3000-Santa Fe, Argentina
e-mail: (jdelia, mstorti, nnigro)@intec.unl.edu.ar
web page: http://venus.ceride.gov.ar/CIMEC

[†]Becario Proyecto FOMEC 1055
Universidad Tecnológica Nacional (UTN), Facultad Regional Santa Fe (FRSF)
Lavaise 610, 3000-Santa Fe, Argentina
e-mail: gfranck@intec.unl.edu.ar,

Key Words: fully developed turbulent flow, channel flow, direct numerical simulation, finite element solution, parallel computing, fluid mechanics

Abstract. *In this work numerical simulations by finite elements are performed for a fully developed turbulent and three-dimensional channel flow. This flow case represents a standard benchmark for validations in turbulent flow research. The computations are carried out by Direct Numerical Simulation (DNS). Structured grids are used for the channel geometry while the flow solver is the PETSc-FEM code. DNS is a time-dependent and three-dimensional numerical solution of the flow equations which are computed as accurately as possible without any turbulence model introduced. Homogeneous turbulence and wall turbulence are the most frequently cases considered in DNS literature. Some turbulence statistics such as friction coefficients, production and viscous dissipation rates, Taylor and Kolmogorov microscales are shown. We compare our results for the flow patterns both with those previously published and with the numerical ones.*
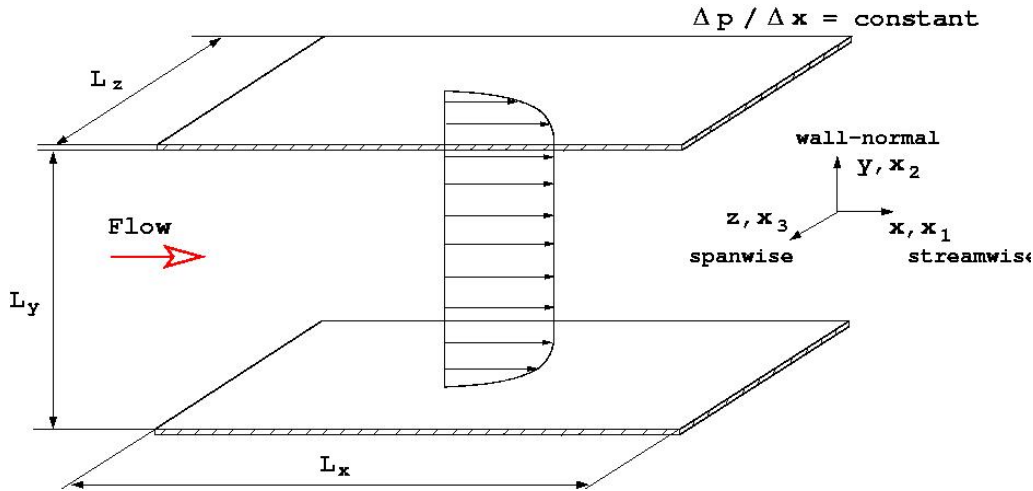
Figure 1: Flow domain for the channel flow, where the channel width is $H = L_y$.

1 INTRODUCTION

Turbulence in fluid flows is a natural phenomenon that cannot be easily defined[1]. However, from a physical point of view there are many common properties of turbulent flows which can be recognized: time and space irregularity, strong mixing, high diffusivity and high vorticity, viscous dissipation, flow structures with continuous spectra of length and time scales, large Reynolds numbers and a three dimensional character, among others. Moreover, there are frequently large scale motions that are organized with some coherent character (e.g. coherent flow structures in a mixing layer or in the wake behind a bluff body), which are flow-dependent and geometry-dependent (e.g. a plane or round jet) and sensitive to inviscid-like instability mechanisms. On the other hand, there are small scale motions that are statistically independent from flow and geometry, but sensitive to the fluid viscosity and with a random and near isotropic behavior.

From a mathematical point of view it is generally accepted that turbulent flows are described by the unsteady Navier-Stokes equations for a viscous fluid. For instance, its applicability has been inferred from the von Kármán-Howarth (VKH) equation that appears in the statistical theories of isotropic turbulence based on correlation methods[2]. In these theories, the unsteady VKH equation is a direct consequence of the Navier-Stokes one when isotropy is assumed, it has been validated in laboratory experiments[3,4] and, it formally describes a diffusion process in a five-dimensional space[5]. Nevertheless, there is not a complete mathematical theory of turbulence as described by the unsteady Navier-Stokes equations, so methods for numerical modeling are often based on heuristics, empiricism and assumptions[6,7].

From a computational point of view, predictive methods in turbulence can be roughly sorted acording to the degree of statistics involved before a numerical solution of the chosen equations is performed[8]:

(i) Direct Numerical Simulation[9] (DNS) of turbulence: where any fluctuating motion in the flow fields is computed from the exact unsteady Navier-Stokes equations, that is, a DNS
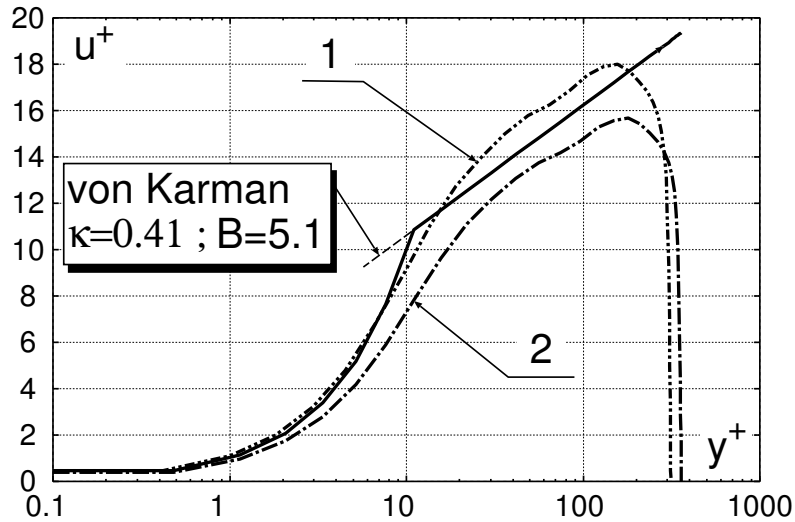
Figure 2: Non-dimensional mean velocity $u^+ = U/U_\tau$ as a function of the non-dimensional wall-normal coordinate $y^+ = yU_\tau/\nu$, when the DNS solution is adimensionalized with: the friction stress τ_w (curve 1) and the limit friction stress $\tilde{\tau}_w$ (curve 2) obtained from Eq. (12).

of turbulence is a time-dependent and three-dimensional numerical solution in which the flow equations are computed as accurately as possible without any turbulence model introduced. Mean flow parameters are later obtained from statistics over a broad set of numerical solutions. DNS considers all degrees of freedom appearing in the flow without using any approximating assumption. However, as the required grid points number increases faster than the square of the Reynolds number, DNS of turbulence is at present feasible only at low or moderate Reynolds numbers;

(ii) Large Eddy Simulations (LES): the large scale motions are computed from the filtered unsteady Navier-Stokes equations while the small-scale ones are modeled with rather *ad hoc* procedures. Then, mean flow parameters are obtained from statistics over a set of solved large-scale motions and small-scale ones (sub-grid modeling);

(iii) Statistical Turbulence Modelling (STM): the whole turbulent motion is assessed through a finite number of statistical parameters, for instance, statistical single-point or two-point moments in the physical or in the Fourier spaces and Probability Density Functions (PDF). However, exact equations governing such statistical parameters are open (the "*closure problem*") due to the non-linearity of the Navier-Stokes equations. Then, additional assumptions are added yielding approximate closed sets of modeled equations, for instance, Reynolds Averaged Navier Stokes equations (RANS), PDF and spectral-closure ones.

The DNS turbulence of channel flow has often been performed in the literature because of its simple geometry, e.g. see Kim *et al.*[10] and Abe *et al.*[11]. The fully developed turbulent channel flow is an example of wall turbulence, that is, turbulence whose structure is mostly
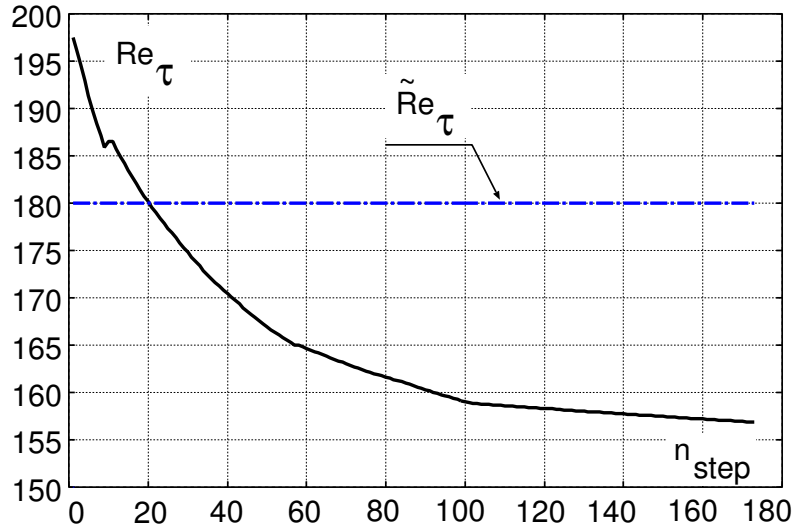
Figure 3: Plot of the friction Reynolds number $\mathrm{Re}_\tau = U_\tau \delta / \nu$ as a function of the time number n, where $\delta = H/2$ is the channel half-width while $\tilde{\mathrm{Re}}_\tau$ is its limit value.
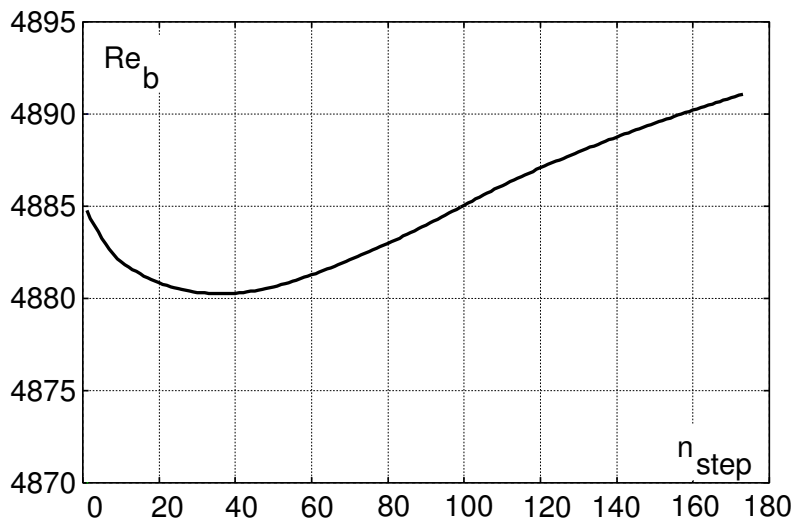
Figure 4: Plot of the bulk Reynolds number $\mathrm{Re}_b = U_b \delta / \nu$ as a function of the time number n, where $\delta = H/2$ is the channel half-width.

influenced by the presence of a solid boundary in a shear flow. Many DNS of turbulence refer to wall bounded flows and have provide useful databases for analysing near-wall effects (see the review article of Friedrich[1] *et al.*).

In this work numerical simulations by finite elements are performed for a fully developed turbulence in a three-dimensional channel. The computations are carried out by Direct Numerical Simulation (DNS) with a structured grid. A main objective is to calibrate a LES model in the PETSc-FEM flow solver[19,20].
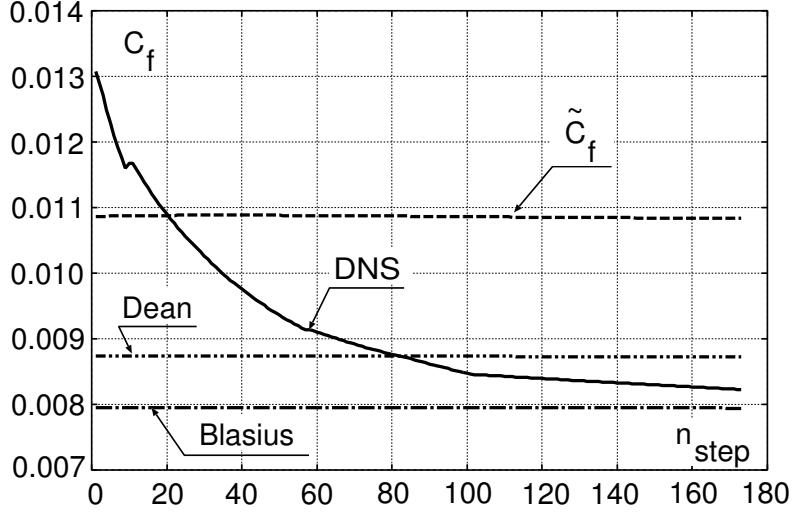
Figure 5: Plot of the friction coefficient C_f as a function of the time number n compared with the correlations of Dean for channel flow, Blasius for pipe flow, and the limit friction value $\tilde{C}_f$.

2 FLOW DOMAIN

A fully developed turbulent flow in a three dimensional channel of rigid and smooth walls is assumed, see Fig. 1, where $x(x_1)$, $y(x_2)$ and $z(x_3)$ are the streamwise, wall-normal and spanwise directions, respectively, and $x = (x, y, z)$. The mean flow is in the x-direction and is driven by a body force γ_x, while the x streamwise and z spanwise directions are assumed as infinites. A fully developed turbulent regime is assumed, with flow velocity $u = u(x, t)$, with $u = (u_x, u_y, u_z)$, which is homogeneous in its time-mean structure in the streamwise direction, where a viscous and incompressible fluid of Newtonian type is employed whose physical properties are taken as constants. The assumed symmetry in the z spanwise direction means only the off-diagonal terms $\langle u_x u_y \rangle_{\Omega,T}$ in the Reynolds stress will be nonzero and it depends only on the y wall-normal direction, where $\langle ... \rangle$ denotes average in the flow domain Ω until some final time T.

3 ROUGH ESTIMATES

As it is well known[12], the Kolmogorov scales of length, time and velocity are given by

$$\eta_K = (\nu^3/\epsilon)^{1/4} \quad ; \quad \Theta_K = (\nu^3/\epsilon)^{1/2} \quad ; \quad u_k = (\nu\epsilon)^{1/4} \quad ; \tag{1}$$

respectively, and

$$\epsilon = 2\nu d \quad ; \quad d = \langle s_{ij} s_{ij} \rangle_{\Omega T} \quad ; \quad s_{ij} = \frac{1}{2}(u_{ij} + u_{ji}) \quad ; \quad u_{ij} = \partial u_i/\partial x_j \, ; \tag{2}$$

where ϵ and s_{ij} are the dissipation and strain rates per unit mass[13], respectively, d is the average of the strain rate square contraction and ν is the fluid kinematic viscosity. On the other hand, two
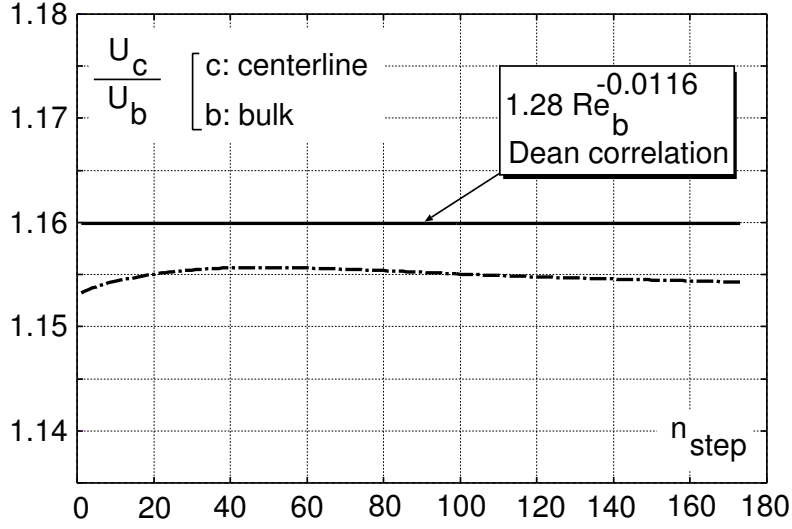
Figure 6: Plot of the ratio of the centerline velocity to the bulk one, U_c/U_b, compared with the Dean correlation $1.28 \, \mathrm{Re_b}^{-0.0116}$, as a function of the time number n.

conditions must meet a DNS of turbulence in order to ensure an adequacy of the results: (i) the length L of the computational domain must be long enough to accommodate the largest eddies, whose typical length is Λ_e, and (ii) the typical grid spacing h must be fine enough to resolve the smallest eddies whose length scale is in the order of the Kolmogorov one. For instance, the grid points number N_{DNS} and the total computational time T_{DNS} in a DNS of homogeneous and isotropic turbulence in a box increase with the Reynolds number as

$$N_{\mathrm{DNS}} \sim \mathrm{Re}_\tau^{9/4} \qquad \text{and} \qquad T_{\mathrm{DNS}} \sim \mathrm{Re}_\tau^{11/4} \ . \tag{3}$$

Assuming that at least 4 nodes in each direction are needed to resolve the smallest eddy, then the grid points number for an uniform spacing h_x can be estimated as

$$N_{\mathrm{uniform}} \approx \left[\frac{\Lambda_e}{\eta_K/4} \right]^3 \ ; \tag{4}$$

and replacing the Kolmogorov length scale η_K given by Eq. (1),

$$N_{\mathrm{uniform}} \approx \left[4\Lambda_e \left(\frac{\epsilon_K}{\nu^3} \right)^{1/4} \right]^3 \ . \tag{5}$$

It is also known[14] that in a channel of width H, the eddies of a fully developed turbulent flow are elongated in the streamwise direction with a scale length $\Lambda_e \approx 2H$. Also, the typical velocity ratio is $U_b/U_\tau \approx 20$ while its dissipation rate is $\epsilon \approx 2U_\tau^2 U_b/H$, where

$$U_b = \lim_{T,\Omega \to \infty} \frac{1}{T\Omega} \int_{\Omega,T} u(x,t) \, d\Omega \, dt \ ; \tag{6}$$

2052
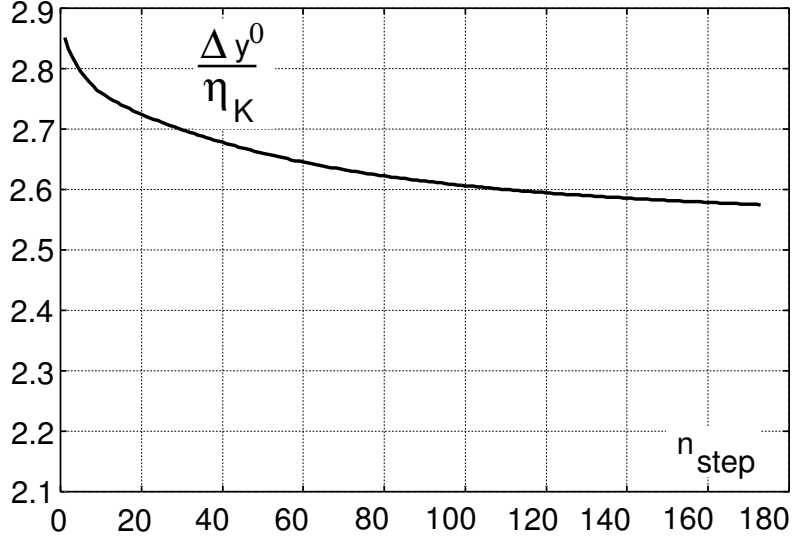
Figure 7: Plot of the ratio of the distance of the first node layer to the Kolmogorov length, $\Delta^0 y/\eta_K$, as a function of the time number n, where $\Delta^0 y = y_1 - y_0$.

is the bulk velocity across the flow domain,

$$U_\tau = \sqrt{\frac{\tau_w}{\rho}} \; ; \tag{7}$$

is the shear velocity,

$$\tau_w = \nu \left. \frac{\partial u}{\partial y} \right|_{\text{wall}} \; ; \tag{8}$$

is the friction stress computed from the DNS results, while ν and ρ are the kinematic viscosity and density of the fluid, respectively. Substituting these estimates into Eq. (5) we have in an uniform mesh of mesh-step h_x that $N_{\text{DNS}} \approx (110 \, \text{Re}_\tau)^{9/4}$, where

$$\text{Re}_\tau = \frac{U_\tau \delta}{\nu} \quad ; \quad \delta = \frac{H}{2} \; ; \tag{9}$$

are the friction Reynolds number and the hydraulic radius for the channel flow case, respectively. From a practical point of view, it is wasteful to use a uniformly-spaced mesh since far wall regions have fairly small dissipation rates ϵ, and then the Kolmogorov length scale η_K is larger there than very near the walls (where the dissipation rate is the biggest). Thus, Kim[10] *et al.* have shown by numerical experiments that with mesh refinement at the walls the factor 110 in Eq. 4 can be replaced by about 3. Thus, a more feasible grid points number order in a DNS of turbulence in channel flow can be estimated as

$$h_x \neq \text{const} \quad \rightarrow \quad N_{\text{DNS}} \approx (3\text{Re}_\tau)^{9/4} \; . \tag{10}$$
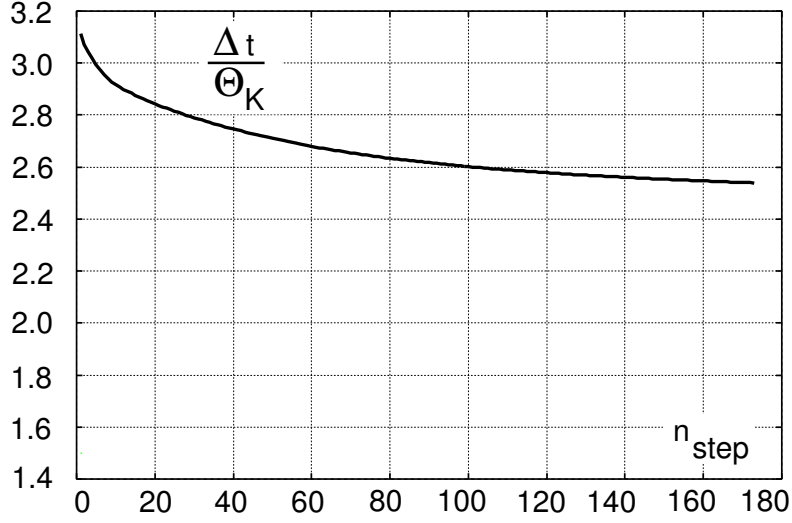
Figure 8: Plot of the ratio of the time-step to the Kolmogorov time scale, $\Delta t/\Theta_K$, as a function of the time number n.

Regarding the time discretization, DNS mostly use explict or semi-implicit methods to overcome severe time-step restrictions due to locally fine grids. Such fine grids arise when the wall-normal velocity gradients must be resolved. Linear stability criteria of explicit schemes lead time steps much lower than the Kolmogorov time scale Θ_K. Another time scale often used as an upper bound in near-wall turbulence is the friction time scale $t_\nu = \nu/U_\tau^2$. For instance, it has been reported that to sustain turbulence is necessary a time step of

$$\Delta t = 0.2 \frac{\nu}{U_\tau^2} \ . \tag{11}$$

When a constant body borce g_x is imposed in the streamwise x-direction of a channel of spanwise width H. A momentum balance on a control volume shows that the limit friction stress is given by

$$\tilde{\tau}_w = \frac{1}{2}\rho g_x H \ . \tag{12}$$

4 AVERAGE PROCEDURE

As in the case of periodic flows, the homogeneity hypothesis in the two infinite directions is assumed[15], that is, all the quantities averaged in these directions are independent of the x-streamwise and z-spanwise directions. Then, by the ergodic hypothesis, the statistical averaged is replaced by an averaging in the x-streamwise and z-spanwise directions given by

$$\overline{f} = \overline{f}(y,t) = \frac{1}{L_x L_z} \int_0^{L_x} \int_0^{L_z} f(x,y,z,t)\,dxdz \ ; \tag{13}$$
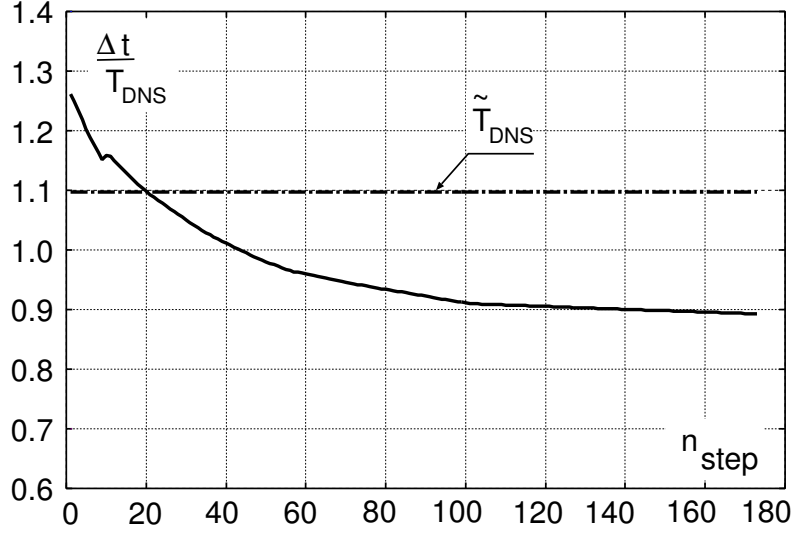
Figure 9: Plot of the ratio of the time-step to the DNS one $\Delta t/T_{\text{DNS}}$ estimed from Eq. (25), as a function of the time number n.

When the simulated flow reaches a statistically steady state, the mean-velocity profile can be defined

$$U(y) = \overline{u}_x(y) = \lim_{T \to \infty} \int_0^T \overline{u}_x(y, t) \, dt \; ; \tag{14}$$

5 MEAN FLOW VARIABLES

In order to characterize the flow in the channel the following mean values are used. The bulk Reynolds number is $\text{Re}_b = U_b \delta/\nu$, where U_b is the mean velocity, while the wall Reynolds number is given by $\text{Re}_\tau = U_\tau \delta/\nu$, where $U_\tau = \sqrt{\tau_w/\rho}$ is the friction velocity, τ_w is the shear stress (statistically averaged) while ν and ρ are the kinematic viscosity and density of the fluid, respectively. The channel half-width $\delta = L_y/2$ is its hydraulic radius (the ratio of the cross sectional area to the transverse wetted perimeter, e.g. see Corcoran[16] *et al.*) which is often used in the literature. The normalized mean velocity and wall-normal coordinate are given by $u^+ = u/U_\tau$ and $y^+ = yU_\tau/\nu$, respectively. The friction coefficient C_f is defined from $\tau_w = C_f(\rho U_b^2/2)$.

6 GOVERNING EQUATIONS

The unsteady Navier-Stokes equations (NS) for the flow of a viscous and incompressible Newtonian fluid are written as

$$\rho \left(\partial_t u + u \cdot \nabla u - f \right) - \nabla \cdot \boldsymbol{\sigma} = 0 \; ;$$
$$\nabla \cdot u = 0 \; ; \tag{15}$$
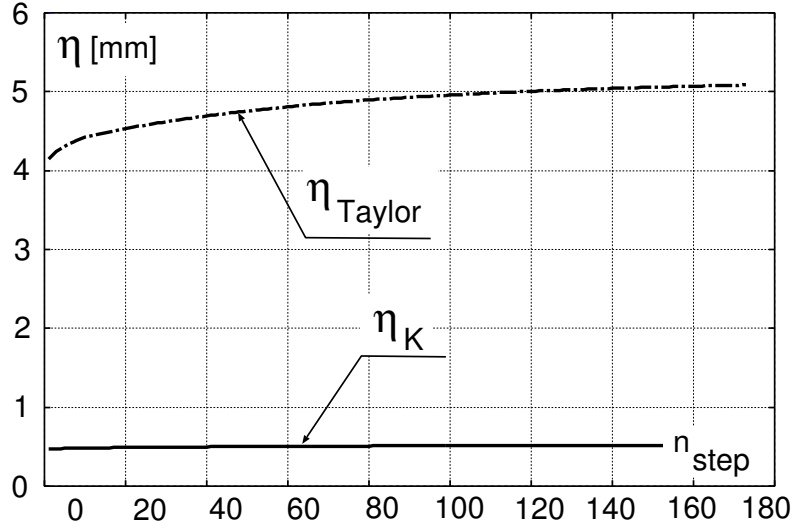
Figure 10: Plots of the Kolmogorov length η_K and and Taylor η_{Taylor} scales as functions of the time number n.

on the flow domain Ω, for all time $t \in [0, T]$ where T is a some final time, u is the fluid velocity, f is the body force and ρ is the fluid density. The fluid stress tensor $\boldsymbol{\sigma}$ is decomposed into its isotropic $-pI$ and deviatoric T parts

$$\boldsymbol{\sigma} = -pI + T \; ; \tag{16}$$

where p is the pressure and I is the identity tensor. As only Newtonian fluids with constant physical properties are considered, its deviatoric part T is related linearly to the strain rate tensor with

$$T = 2\mu\boldsymbol{\epsilon} \quad ; \quad \boldsymbol{\epsilon} = \frac{1}{2}\left[\nabla v + (\nabla v)^T\right] \; ; \tag{17}$$

where μ and $\nu = \mu/\rho$ are the dynamic and kinematic viscosity of the fluid and $(...)^T$ denotes the transpose. In channel flow periodic boundary conditions are imposed in the x-streamwise and z-spanwise directions (or at the boundary of the xz-horizontal planes) as

$$\begin{aligned}
u(x + L_x, y, z, t) &= u(x, y, z, t) \; ; \\
u(x, y, z + L_z, t) &= u(x, y, z, t) \; ; \\
p(x + L_x, y, z, t) &= p(x, y, z, t) \; ; \\
p(x, y, z + L_z, t) &= p(x, y, z, t) \; ;
\end{aligned} \tag{18}$$

while no-slip ones for the velocity

$$u(x, 0, z, t) = u(x, L_y, z, t) = 0 \; ; \tag{19}$$

are imposed on the top and bottom walls for all time $t \in [0, T]$. The lengths L_x and L_z are the assumed periods in the two infinite directions x-streamwise and z-spanwise large enough to accommodate the largest eddies.
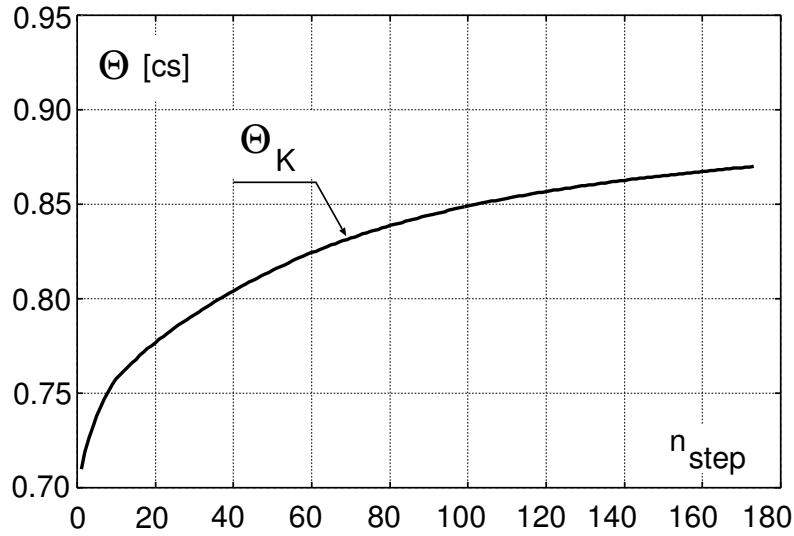
Figure 11: Plot of the Kolmogorov time Θ_K scale as a function of the time number n.

7 NUMERICAL SOLUTION BY FINITE ELEMENTS

The numerical simulation is performed by a stabilized finite element scheme where, at each node and at each time step, the moment and continuity equations are solved for the three components of velocity and pressure. The combined Streamline Upwind Petrov Galerkin (SUPG) and Pressure Stabilized Petrov Galerkin (PSPG)] scheme, proposed by Tezduyar[17,18] *et al.* is employed for stabilization of the advective and incompressibility terms. This combined scheme is due to two distinctive difficulties in the numerical resolution of the Navier-Stokes equations of flows of incompressible and viscous fluids by finite elements. First, when the Reynolds number increases, these equations are more dominated by the advection term. On the other hand, the incompressibility condition is not really a evolution equation itself but, rather, a restriction one on the velocity field. This implies, in turn, that only some combinations of the velocity and pressure interpolation spaces can be employed, that is, those that satisfy the Brezzi-Babuska condition. The spatial discretization has equal order for pressure and velocity (linear tetrahedral elements), and is stabilized through the addition of two operators. Advection at high Reynolds numbers is stabilized with the SUPG operator, while the PSPG one stabilizes the incompressibility condition, which is responsible of the checkerboard pressure modes. When the modified equations are then discretized by finite elements in space, an Ordinary Differential Equation (ODE) system in time results, which is next discretized by a finite difference method and, at each time step, we have a non-linear system of equations

$$F\left(\frac{u^{n+1} - u^n}{\Delta t}, p^{n+1}\right) = 0 \ . \tag{20}$$

Then, having the state of the fluid at time t^n, we solve the velocity and pressure unknowns at time t^{n+1}.

2057
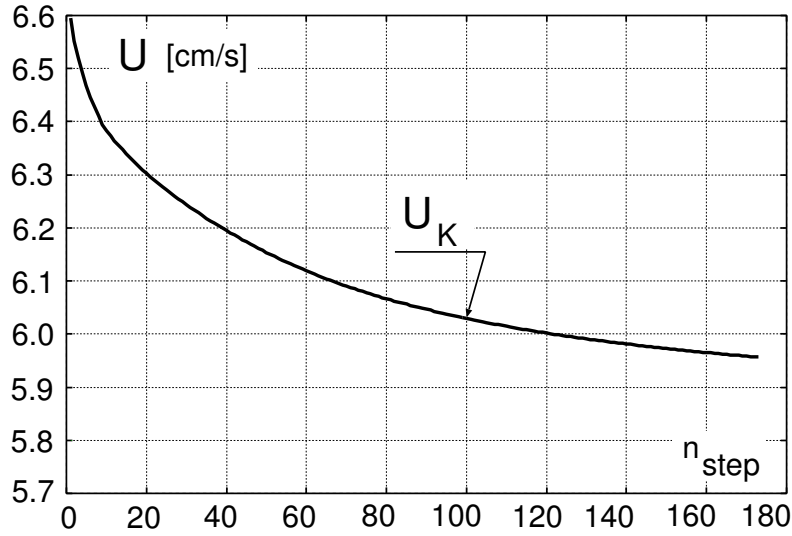
Figure 12: Plot of the Kolmogorov velocity U_K scale as a function of the time number n.

The whole strategy is implemented within the PETSc-FEM[19,20] code, a multi-physics finite element library. In our DNS simulations we have used its special matrix solver "Interface Iterative and Sub-domain Direct" (IISDMat), which solves the linear system by iteration over the interface nodes while a direct method is employed in each interior sub-domain (this is commonly referred as a "Domain Decomposition Method"). The PETSc-FEM code is based on MPI[21] (Message Passing Interface) and PETSc[22] (Portable Extensible Toolkit for Scientific computations), a scientific library that gives to the developer a parallel environment with different levels of complexity.

8 COMPUTATIONAL PARAMETERS

The computational flow domain is the box $\Omega = [0, L_x] \times [0, L_y] \times [0, L_z] \times$, where $L_x = \pi$ is the streamwise length, $L_y = 1$ is the channel width and $L_y = H = \pi/2$ its spanwise width. The lengths L_x and L_z are chosen in order to ensure that the turbulence fluctuations are uncorrelated at one half-period of separation. A structured finite element mesh with linear tetrahedral elements is employed. It is resolved by an equidistant grid in the xz-planes, with $N_x = 128$ and $N_z = 64$ points along streamwise and spanwise directions, respectively. In order to verify Eq. (10) the mesh step should be 40% smaller. Along the wall-normal y direction, a non-equidistantly grid is placed with $N_y = 34$ points along wall-normal direction, with refinement center/wall ratio of $h_{ratio} = 75$, where the first point at $y^+ = 0.48$. There is a total of $N_x \approx 294$ K-nodes and $N_u \approx 1.18$ M-degree of freedom. In order to obtain a wall Reynolds number $\mathrm{Re}_\tau \approx 180$ and mean velocities $O(1)$, the kinematic viscosity was set to $\nu = 3 \ 10^{-5} \ \mathrm{m}^2/\mathrm{s}$ and the body force $g_x = 0.00025 \ \mathrm{N/m}^3$.

The overall computation was performed by continuation on the body force g_x (related to the friction Reynolds number), which was started with a laminar velocity profile. The final Courant
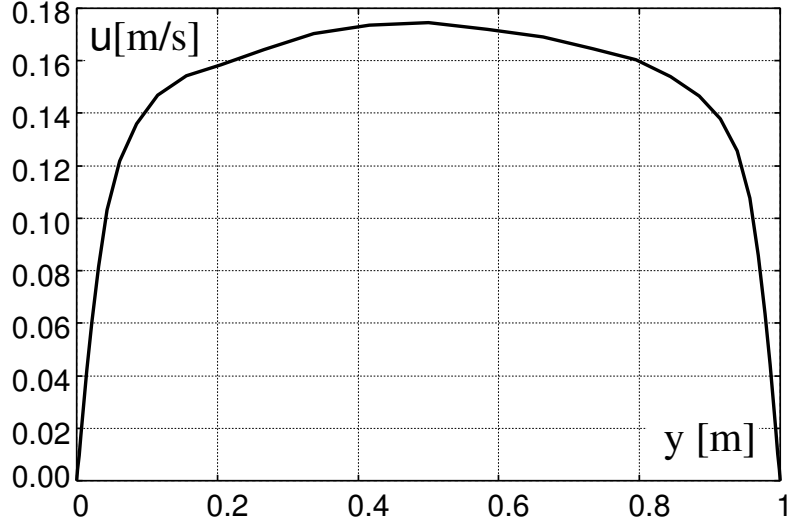
Figure 13: Mean velocity U_x as a function of the wall-normal coordinate y.

number was $N_C \approx 0.5$ and the last time-step $\Delta t = 0.002$ s. This final time-step is lower than the viscous one from the estimate given by Eq. (11).

9   NUMERICAL RESULTS

The DNS curves are adimensionalized with both the friction stress τ_w (computed from Eq. 8) and the asymptotic friction stress $\tilde{\tau}_w$ (given by Eq. 12).

Fig. 2 shows plots of the non-dimensional mean velocity $u^+ = u/u_\tau$ as a function of the non-dimensional wall-normal coordinate $y^+ = yu_\tau/\nu$. As it is well known, in fully developed turbulence there is a logarithmic region empirically approximated by

$$u^+ = A \ln y^+ + B \; ; \tag{21}$$

where $A = 1/\kappa$ is the reciprocal of the von Kármán parameter and B is an additive one. Several values are found in literature (for both smooth and rough walls) and we have chosen $\kappa = 0.41$ and $B = 5.1$.

Plots of the friction Reynolds number $\mathrm{Re}_\tau = U_\tau \delta/\nu$ and bulk Reynolds number $\mathrm{Re}_b = U_b \delta/\nu$, as functions of the time number n are shown in Figs. 3 and 4, respectively, where $\delta = H/2$ is the channel half-width (the hydraulic radius for this case).

Plots of the friction coefficients C_f as functions of the time number n are shown in Fig. 5 obtained with: (i) the present DNS, (ii) the Dean empirical correlation for channel flow

$$C_f = 0.073 \, \mathrm{Re}_b^{-0.25} \; ; \tag{22}$$

and (iii) the Blasius one for pipe flow

$$C_f = 0.079 \, (2\mathrm{Re}_b)^{-0.25} \; . \tag{23}$$
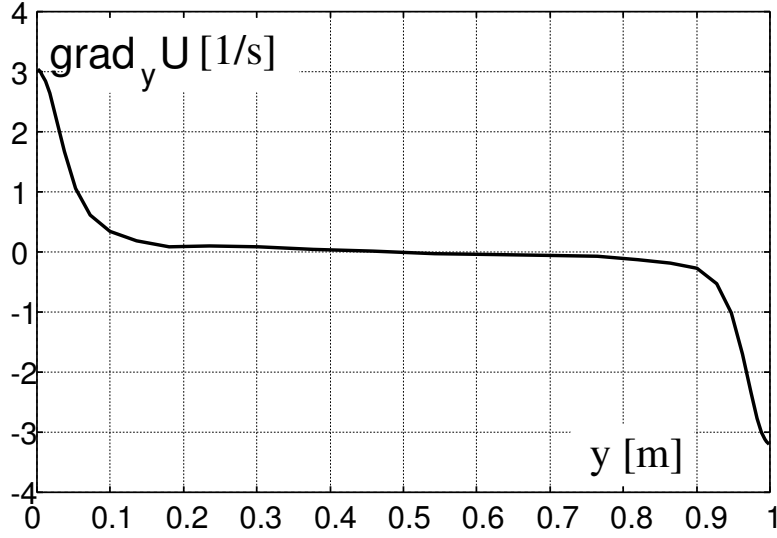
Figure 14: Mean velocity gradient $\partial U_x/\partial y$ as a function of the wall-normal coordinate y.

A plot of the ratio of the centerline velocity to the bulk one, U_c/U_b, as a function of the time number n, compared with the Dean correlation

$$\frac{U_c}{U_b} = 1.28 \, \mathrm{Re_b}^{-0.0116} \; ; \tag{24}$$

is shown in Fig. 6.

A plot of the ratio of the distance of the first node layer to the Kolmogorov length $\Delta^0 y/\eta_K$, where $\Delta^0 y = y_1 - y_0$, is shown in Fig. 7, and another for the ratio of time-step to the Kolmogorov time $\Delta t/\Theta_K$ is shown in Fig. 8, both as functions of the time number n. A plot of the ratio of the time-step to an estimative DNS one, $\Delta t/T_{\mathrm{DNS}}$, is shown in Fig. 9 as a function of the time number n, where (e.g. see Wilcox[14])

$$T_{\mathrm{DNS}} = 0.003 \, \frac{H}{U_\tau \sqrt{\mathrm{Re_\tau}}} \; . \tag{25}$$

Plots of the Kolmogorov scales for length η_K, time Θ_K and velocity U_K computed by Eq. 1 are shown in Figs. 10, 11 and 12, respectively, all as functions of the time number n. In Fig. 10, as a reference, the Taylor scale

$$\eta_{\mathrm{Taylor}} = \sqrt{15 \, \nu \, \frac{U_b^{\,2}}{\epsilon}} \; ; \tag{26}$$

for homogeneous and isotropic turbulence, it is also ploted as a function of the time number n, where it is verified that $\eta_K < \eta_{\mathrm{Taylor}}$.

The last mean velocity U_x and mean velocity gradient $\partial U_x/\partial y$ as functions of the wall-normal coordinate y are shown in Figs. 13 and 14, respectively.

The mean dissipation rate ϵ as a function of the wall-normal coordinate y is shown in Fig. 15.
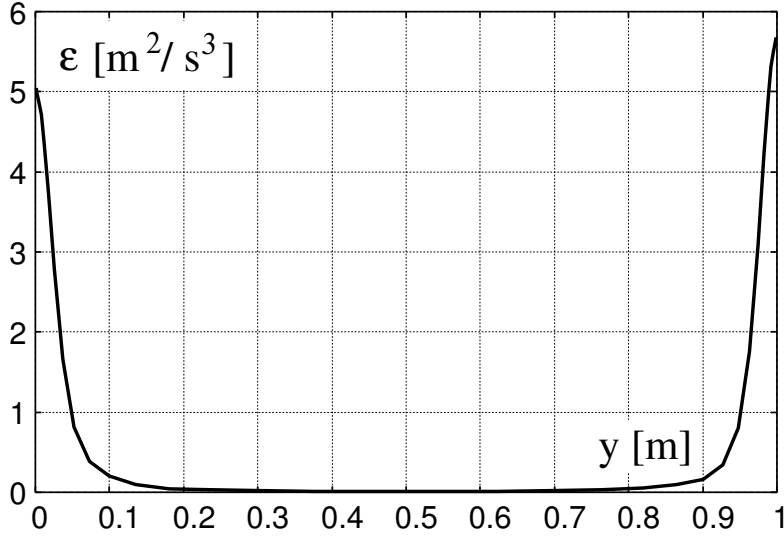
Figure 15: Mean dissipation ϵ as a function of the wall-normal coordinate y.

10 DISCUSSION

Due to the fact that the mesh is not properly refined in the sense that the mesh step should be 40% smaller in order to verify Eq. (10), an assessment is necessary in order to clarify if the present simulation is more likely a LES without a subscale model than a truly DNS. To quantify this possibility an analysis beyond the mean flow should be made. For this aim, the external work $W_e = \rho g_x U_b \Omega$ should be equal in mean to the dissipation energy

$$E_d = \int_\Omega \epsilon \, d\Omega = \int_{L_y} \langle \epsilon \rangle_{L_x L_z} \, dy \; ; \tag{27}$$

where

$$\langle \epsilon \rangle_{L_x L_z} = \frac{1}{L_x L_z} \int_{L_x} dx \int_{L_z} \epsilon(x, y, z) \, dz \; ; \tag{28}$$

both W_e and E_d are integrated in the flow volume $\Omega = L_x L_y L_z$. Fig. 16 shows a plot of the external work W_e and dissipation energy E_d in the flow volume Ω, as a function of the time number n. From this figure it can inferred that (i) the difference between dissipation and external work it is not small enough, (ii) that the external work is bigger than the dissipation energy due to the numerical dissipation added by the numerical method and (iii) the relative numerical dissipation is $BC/AC \approx 30\%$. It can be concluded that the present simulation is more likely to be a LES without a subscale model than a truly DNS. For a truly DNS the mesh step should be more refined. For instance, the number of nodes should be increased from the ≈ 300 K-nodes in the present simulations to 600 and 900 K-nodes. In this way a convergence test under mesh refinement could be also performed.

Another validation is to compute spatial and time correlations of the fluctuating velocities, which are more sensitive to the subscale models than the mean ones. For this aim, the Reynolds
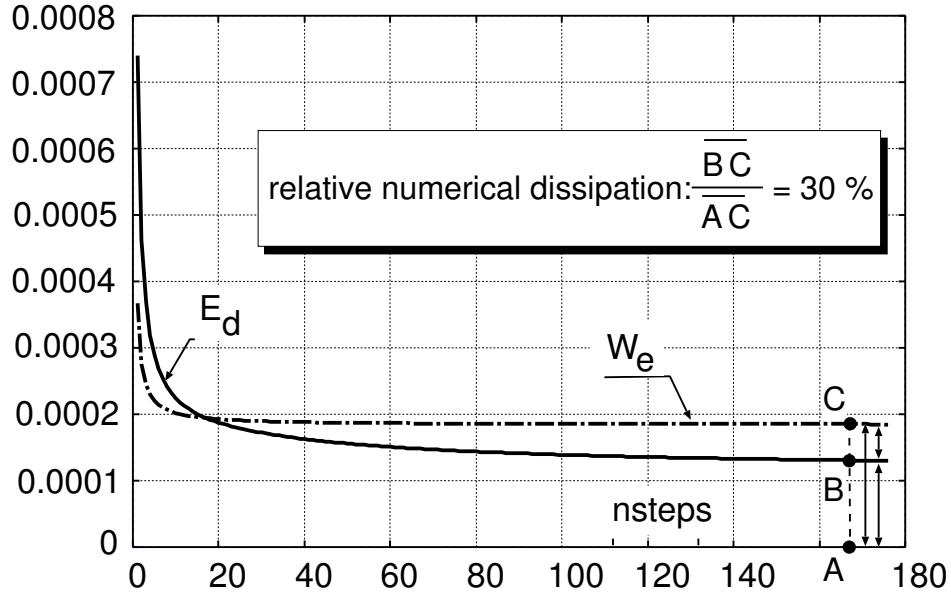
Figure 16: External work $W_e = \rho g_x U_b \Omega$ and viscous dissipation $E_d = \int_\Omega \epsilon d\Omega$ integrated in the volume $\Omega = L_x L_y L_z$ as a function of the time number n.
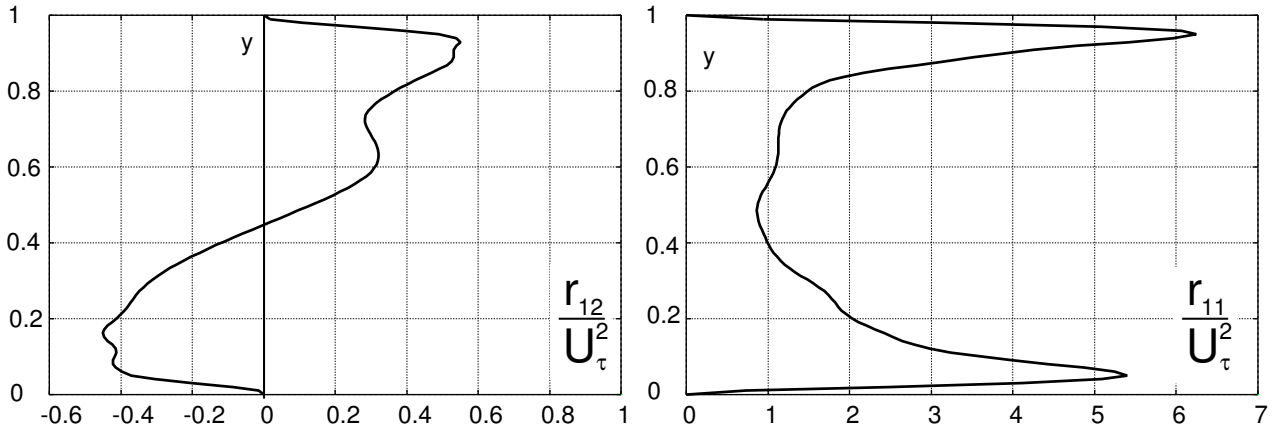
Figure 17: Reynolds stresses $r_{12} = \rho\langle\tilde{u}_1\tilde{u}_2\rangle$ and $r_{11} = \rho\langle\tilde{u}_1\tilde{u}_1\rangle$ as a function of the wall-normal coordinate y.

stresses $r_{11} = \rho\langle\tilde{u}_1\tilde{u}_1\rangle$ and $r_{12} = \rho\langle\tilde{u}_1\tilde{u}_2\rangle$ can be computed as a function of wall-normal coordinate y, where $\tilde{u}_i = u_i - U_i$ is the fluctuating velocity, while u_i and U_i are the instantaneous and mean velocities along the i-Cartesian coordinate, respectively. A plot of these Reynolds stresses as a function of the wall-normal coordinate y is shown in Fig. 17.

11   CONCLUSIONS

As Karniadakis[23] remarks, there are two major challenges today in DNS of turbulence: (i) the maximum Reynolds number feasible in numerical simulations is still much lower than those of practical interest and (ii) complicated flow geometries are still untackled. Nevertheless, from a

practical standpoint, statistics computed from the DNS results can be used to test and calibrate closure models and Sub-Grid-Scale (SBS) ones, which are often used to predict the more usual complicated flows of technical interest. Thus, DNS of turbulence is still devoted to flow research since it gives more detailed mechanisms of fluctuating fields and it can be used as a tool to study the turbulence physics. DNS of turbulence can also be considered as an additional source of experimental-like data if is seen as an unobtrusive measuring technique as well for obtaining information about near unmeasurable properties like pressure fluctuations. Other test cases could be the DNS of turbulence through partially permeable pipes since it has been reported to behave similarly to flow through rough pipes[24].

Acknowledgments

REFERENCES

[1] Friedrich R., Huttl T.J., Manhart M., and Wagner C. Direct numerical simulation of incompressible flows. *Computers and fluids*, **30**, 555–579 (2001).

[2] Panchev S. *Random functions and turbulence*. Pergamon Press, Hungary, (1971).

[3] Stewart R.W. *Triple velocity correlation in isotropic turbulence*, volume 47. Proc. Cambr. Phil. Soc., (1951).

[4] Towsend A.A. *The structure of turbulent shear flow*. Cambridge Univ. Press, (1956).

[5] Hinze J.O. *Turbulence*. McGraw-Hill, New York, 2nd edition, (1975).

[6] Guermond J.L., Oden J.T., and Prudhomme S. Mathematical perspectives on large eddy simulation models for turbulent flows. Draft version, (June 2002).

[7] Doering C.R. and Gibbon J.D. *Applied analysis of the Navier-Stokes equations*. Cambridge Univ. Press, (1995).

[8] Chassaing P. First glance to turbulence. In *Variable density turbulent flows*, Barcelone, (2003). I.S.S.

[9] Moin P. and Mahseh K. Direct numerical simulation: a tool in turbulence research. *Ann. Rev. Fluid Mech.*, pages 359–378 (1998).

[10] Kim J., Moin P., and Moser R. Turbulence statistics in fully developed turbulent channel flow at low Reynolds number. *Journal of Fluids Mechanics*, **177**, 133–166 (1987).

[11] Abe H., Kawamura H., and Matsuo Y. Direct numerical simulation of a fully developed channel flow with respect to the Reynolds number dependence. *Journal of Fluids Engineering*, **123**, 382–393 (2001).

[12] Monin A.S. and Yaglom A.M. *Statistical Fluid Mechanics*, volume 1-2. MIT Press, 3rd edition, (March 1977). QA 911 / M749 / Inv. 3413.

[13] Tennekes H. and Lumley J.L. *A First Course in Turbulence*. MIT Press, (March 1972).

[14] Wilcox D.C. *Turbulence Modeling for CFD*. DCW, 2nd edition, (1998). ISBN: 0963605151.

[15] Bouchon F. and Jauberteau F. A multilevel method applied in the nonhomogeneous direction of the channel flow problem. *Applied numerical Mathematics*, pages 1–34 (2001).

[16] Corcoran W.M., Opfell J.B., and Sage B.H. *Momentum Transfer in Fluids*. Academic Press, (1956).

[17] Tezduyar T., Mittal S., Ray S., and Shih R. Incompressible flow computations with stabilized bilinear and linear equal order interpolation velocity-pressure elements. *Comp. Meth. Applied Mechanics and Engineering*, **95**(95), 221–242 (1992).

[18] Güler I., Behr M., and Tezduyar T. Parallel finite element computation of free-surface flows. *Computational Mechanics*, **23**(2), 117–123 (1999).

[19] Sonzogni V.E., Yommi A., Nigro N., and Storti M. Cfd finite element parallel computations on a beowulf cluster. In *European Congress on Computational Methods in Applied Sciences and Engineering, ECCOMAS 2000*, (11-14 September 2000).

[20] PETSc-FEM: A general purpose, parallel, multi-physics FEM program. GNU General Public License (GPL), http://minerva.arcride.edu.ar/petscfem.

[21] Message passing interface (MPI). http://www.mpi-forum.org/docs/docs.html.

[22] Balay S., Gropp W., McInnes L.C., and Smith B. Petsc 2.0 users manual. Technical Report UC-405, Argonne National Laboratory. Mathematics and Computer Science, (1997).

[23] Karniadakis G.E. Simulating turbulence in complex geometries. *Fluid Dynamics Research*, **24**, 343–362 (1999).

[24] Wagner C. and Friedrich R. DNS of turbulent flow along passively permeable walls. *Heat and fluid flow*, **21**, 489–498 (2000).